Supplementary Material to the article "What can we learn from nonequilibrium response of a strange metal?"

We solve a problem of current spreading in a layered two-dimensional geometry with poor interface. The results evidence that the contact resistance scales similar to the resistivity of the parent film. Numerical simulations are performed to understand possible impact of the interface resistance in [1]. The experimental deviations could be expained by such a contact effect.

LAYOUT

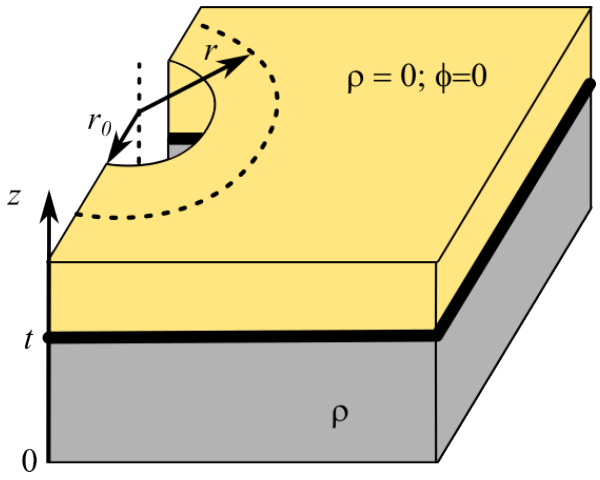

Fig. S1. Sketch of a layered contact. Lower grey layer has a finite resistivity (thickness t). Upper yellow layer is an ideal metal, which is grounded. A very thin interface between the two layers is depicted by a black thick line. The interface emulates bad contact and in the presence of current there is a finite voltage drop across the interface.

Fig. S1 represents a model of a layered contact. The upper layer is an ideal metal with infinite conductivity, which is grounded, i.e. its electric potential is $\phi = 0$. The lower layer is a metal with finite conductivity $\sigma = 1/\rho$ and thickness t. The interface between the two metal layers is assumed to have zero thickness and is characterized by a finite conductivity per unit area σ_i. The current inflows the lower layer at the inner radial contact of the radius r_0. The center of that inner contact is chosen to be the origin of a cylindrical polar coordinate system (r, φ, z).

QUALITATIVE PICTURE

A good estimate of the spreading resistance can be achieved with the following argument. Consider the contact of geometry of Fig. S1 with the inner and outer radii of r_0 and $r_{max} \gg r_0$, respectively. For $\sigma_i = 0$ the current does not flow over the interface and remains in the lower layer. In this case, the contact resistance has a log-divergence in size: $R_1(r_{\max}) = \rho(\pi t)^{-1} \ln(r_{\max}/r_0)$. On the other hand, if all the voltage drop occurs across the interface between the two layers, which happens for $\rho = 0$, the contact resistance is $R_2(r_{\max}) = 2(\pi r_{\max}^2 \sigma_i)^{-1}$. In an infinite contact with both ρ and σ_i non-zero, the current overflows the interface within the region of the radius given by the current transfer length λ. This length can be estimated from $R_1(\lambda) = R_2(\lambda)$. For such λ, the contact resistance can be estimated as:

$$R_c \approx R_1(\lambda) = \frac{\rho}{\pi t} \ln(\lambda/r_0) \tag{S1}$$

SOLUTION: HALF-PLANE INFINITE PAD

The spatial distribution of the electric potential is found from a solution of Laplace's equation $\Delta\phi = 0$. Owing to the axial symmetry, the potential is independent of φ and we find the solution of the form $\phi(r, z) = F(r)G(z)$. It then follows from the Laplace's equation:

$$\frac{1}{F}\frac{d^2F}{dr^2} + \frac{1}{rF}\frac{dF}{dr} = -\frac{1}{G}\frac{d^2G}{dz^2}, \tag{S2}$$

which implies that the rhs and lhs of this equation equal the same constant, independent of both r and z. This equation is supplemented by the expressions for the current density in the lower metal layer:

$$j_z = -\sigma F(r)\frac{dG}{dz} \tag{S3}$$

$$j_r = -\sigma G(z)\frac{dF}{dr} \tag{S4}$$

The solution for $G(z)$ is straightforward. Assuming $d^2G/dz^2 = -\gamma^2 G(z)$ and from the boundary condition of $j_z = 0$ at the $z = 0$ plane, we find $G(z) = G_0 \cos(\gamma z)$. The boundary condition at the interface $z = t$ is different. We assume that the interface between the two metals has zero thickness and is characterized by a finite conductivity per unit area σ_i. Hence, the finite voltage drop at the interface is connected to the current density along the z-axis:

$$\phi(r, z = t - 0) - \phi(r, z = t + 0) = \frac{j_z(r, z = t)}{\sigma_i},$$

where, by assumption, $\phi(r, z = t + 0) = 0$. Together with the solution for $G(z)$ and Eq. (S3) this expression determines γ:

$$\gamma \tan(\gamma t) = \frac{\sigma_i}{\sigma}, \tag{S5}$$

which in the limit of $\gamma t \ll 1$ reduces to $\gamma = \sqrt{\sigma_i/(t\sigma)}$. Note that γ^{-1} has a meaning of current transfer length, i.e. a typical length on which most of the current from the lower layer flows over to the upper layer. Going back to the Eq. (S2), the solution for $F(r)$ is found from:

$$x\frac{d^2F}{dx^2} + \frac{dF}{dx} - xF = 0, \tag{S6}$$

where $x = \gamma r$. The solution of (S6) converging at $x \to \infty$ is $F(r) = F_0 K_0(\gamma r)$, where K_0 is the Bessel-K function of the zero-th order. From the identity $dK_0(x)/dx = -K_1(x)$, where K_1 is the Bessel-K function of the first order, one finds a solution for the electric potential and radial current density:

$$\phi(r,z) = \phi_0 K_0(\gamma r)\cos(\gamma z) \tag{S7}$$
$$j_r(r,z) = \phi_0 \gamma\sigma K_1(\gamma r)\cos(\gamma z), \tag{S8}$$

where $\phi_0 = F_0 G_0$ is a constant. The resistance R_c of the contact pad depicted in Fig. S1 is calculated easily for $\gamma t \ll 1$. The total current flowing into the contact equals $I = \pi r_0 t \cdot j_r(r = r_0)$, so that:

$$R_c = \frac{1}{\pi\sigma t}\frac{K_0(\gamma r_0)}{\gamma r_0 K_1(\gamma r_0)}, \tag{S9}$$

with $r_0 = w/2$, where w is the width of a wire to which the contact pad is attached. Using that $K_0(x)/xK_1(x) \approx \ln(1.12/x)$ in the limit of $x \to 0$, one can simplify the Eq. (S9) for $\gamma w \ll 1$:

$$R_c \approx \frac{\rho}{\pi t}\ln\left(\frac{2.24}{\gamma w}\right) \tag{S10}$$

The Eq. (S10) shows that in the case of poor interface ($\gamma w \ll 1$) the contact resistance scales proportional to the material's resistivity ρ. The dependence of γ on σ, see Eq. (S5), is has a minor effect and enters via the log-term. Note that (S10) is very close to the qualitative estimate of (S1) with $\lambda \approx \gamma^{-1}$.

SOLUTION: FINITE HORN-SHAPED PAD

Consider a more realistic geometry of the finite size contact pad that has a shape of a horn. The angular width of the horn is θ and the inner and outer radii are, respectively, r_0 and $r_{\max}$, see the Fig. S2. In this case the solution of the Eq. (S6) is found from a different boundary condition, namely from $j_r(r = r_{\max}) = 0$, i.e. zero in-plane current at the outer biundary of the lower layer. In this case $G(z)$ is the same and $F(r)$ becomes a superposition of the two Bessel functions. The expressions for the electric potential and current density are:

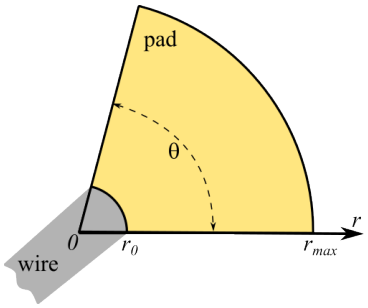

Fig. S2. Sketch of a realistic contact pad, shaped as a horn with the inner radius of r_0 and the outer radius of $r_{\max}$. The color notations are the same as in Fig. S1.

$$\frac{\phi(r,z)}{\phi_0} = \cos(\gamma z)\left[K_0(\gamma r) + \frac{K_1(\gamma r_{\max})}{I_1(\gamma r_{\max})}I_0(\gamma r)\right] \tag{S11}$$
$$\frac{j_r(r,z)}{\phi_0\gamma\sigma} = \cos(\gamma z)\left[K_1(\gamma r) - \frac{K_1(\gamma r_{\max})}{I_1(\gamma r_{\max})}I_1(\gamma r)\right], \tag{S12}$$

where I_0 and I_1 are the Bessel-I functions of the zero-th and first order. In the limit of $r_{\max} \gg \gamma^{-1}$ the solution coincides with that for an infinite contact pad. The resistance of the contact pad of Fig. S2 is given by:

$$R_c = \frac{1}{\theta\sigma t x_0}\frac{K_0(x_0)I_1(x_{\max}) + I_0(x_0)K_1(x_{\max})}{K_1(x_0)I_1(x_{\max}) - I_1(x_0)K_1(x_{\max})}, \tag{S13}$$

where $x_0 = \gamma r_0$ and $x_{\max} = \gamma r_{\max}$ and θ in the denominator takes into account the angular width of the horn. For $x_0 \ll x_{\max}$, $K_1(x_0)I_1(x_{\max}) \gg I_1(x_0)K_1(x_{\max})$ and the Eq. (S13) simplifies:

$$R_c = \frac{1}{\theta\sigma t x_0}\left[\frac{K_0(x_0)}{K_1(x_0)} + \frac{I_0(x_0)K_1(x_{\max})}{K_1(x_0)I_1(x_{\max})}\right] \tag{S14}$$

For $x_{\max} \gg 1$ the contact pad size is much larger than γ^{-1} and the second term in the brackets vanishes exponentially. In this case the result for R_c reproduces (S9) with θ instead of π in the denominator, which is a result of reduced angular width. More interesting is the case the pad size smaller than the current transfer length, $x_0 \ll x_{\max} < 1$. Using the asymptotic approximations $I_0(x_0) \approx 1$, $K_0(x_0) \approx \ln(1.12/x_0)$, $K_1(x_0) \approx 1/x_0$, $I_1(x_{\max}) \approx x_{\max}/2$ and $K_1(x_{\max}) \approx 1/x_{\max}$, we find:

$$R_c = \frac{\rho}{\theta t}\ln\left(\frac{1.12}{\gamma r_0}\right) + \frac{1}{A_c\sigma_i}, \text{ with } A_c = \theta r_{\max}^2/2 \tag{S15}$$

Expression (S15) shows that the resistance of a contact pad with $r_0 \ll r_{\max} < \gamma^{-1}$ has an extra contribution equal to the total interface resistance of the pad with the area of A_c. It is easy to see, that for $\sigma \to \infty$ ($\rho \to 0$) one has $\gamma \to 0$ and (S15) reduces to $R_c = (A_c\sigma_i)^{-1}$, that is the contact resistance between two ideal conductors is controlled solely by the interface resistance.

NUMERICAL MODELING

Finite interface resistance could explain substantial deviation in resistivity of two nanowire devices in [1]. The resistivity of the 0.66 μm long wire is roughly an order of magnitude higher, as compared to the 28 μm long wire. Based on their response to the temperature and magnetic field similar to those of the parent film it is argued that this deviation is not a result of the contact resistance. The above calculations indicate that this argument has a caveat.

As follows from (S10), the resistance of an infinite contact pad with a poor interface between the layers has nearly identical to the parent material temperature (T) response, since $R_c \propto \rho$ up to an unimportant log-factor. The same is expected to hold also for the magnetic field response. For a finite pad a constant resistance offset is present, according to (S15). We have performed numerical calculations of realistic device layouts in order to understand possible effects of the interface conductivity and contact area on the temperature dependence of the resistivity in the smaller nanowire.

Fig. S3 (upper panel) shows the T-dependence of the resistance of the smaller wire with dimensions $L = 0.66$ μm (length), $w = 0.24$ μm (width) and $t = 60$ nm (film thickness). Circles mark the measured resistance and crosses correspond to $R_0 = \rho L/(wt)$, expected from the resistivity measured in the 28 μm long wire under the assumption of ideal interface ($\sigma_i = \infty$). This data is obtained by digitizing the published data. In order to capture the experimental behavior of the smaller wire we performed numerical simulations for two sizes of the contact pads, shaped as close as possible to the original design. The designs of a bigger (pads-I) and smaller (pads-II) contact pads are shown in the lower panel of Fig. S3. Numerical results are shown in Fig. S3 by dashed-dotted and dashed black lines, respectively, both obtained assuming the interface conductance of $\sigma_i = 4.7 \cdot 10^6\,\mathrm{S/m}$. The values of σ_i, ρ and t correspond to the current transfer length of $\gamma^{-1} \approx 280\,\mu$m, which is comparable to the size of pads-I and considerably larger than the size of pads-II. The total device resistance $R = R_0 + 2R_c$ is much larger than R_0 (crosses) and exhibits sizable T-dependence, comparable to the experiment (circles). The resistance is larger for pads-II, as expected for their smaller area according to (S15). Moreover, the experiment is consistent with the prediction of (S13) for $r_0 = w/2$, $r_{\max} = 500\,\mu$m and $\theta = \pi/2$, see the red dotted line. Altogether, we find that poor interface quality can well be responsible for the unexpectedly high resistance of the smaller device.

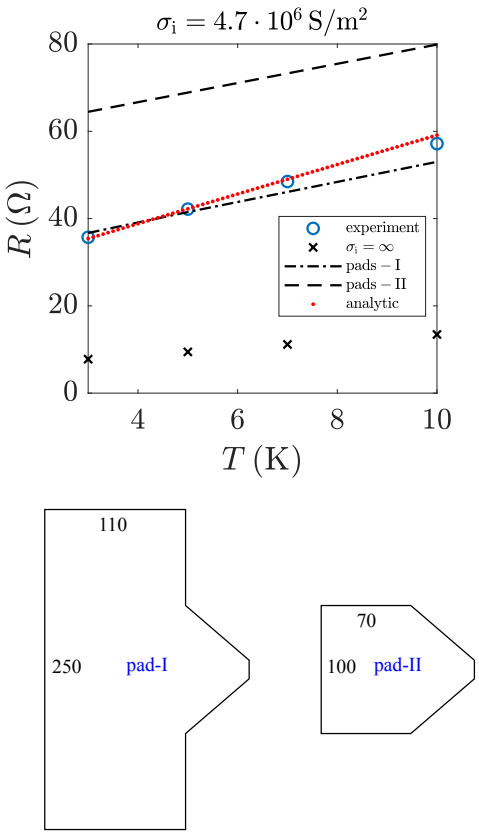

Fig. S3. (upper panel): T-dependence of the resistance in a smaller wire. Circles mark the measured resistance and crosses correspond to $R_0 = \rho L/(wt)$, expected from the resistivity measured in the 28 μm long wire under the assumption of ideal interface ($\sigma_i = \infty$). The theoretical fits take into account the contact resistance via $R = R_0 + 2R_c$. Red dotted line is the analytical result (S13) for $r_0 = w/2$, $r_{\max} = 500\,\mu$m and $\theta = \pi/2$. Black lines are numerical simulations for the contact pads designs pads-I and pads-II. (lower panel): sketches of the designs used in numerics.

SUMMARY

We observed that in the two-dimensional case the resistance of a contact pad caused by poor interface quality scales nearly proportional to the resistivity of a parent film. This could explain deviations in resistivity values between the larger and smaller devices in the experiments of [1]. The observation has important consequence for the interpretation of shot noise data in a smaller wire, since the effective length of the device may exceed the electron-phonon relaxation length. In this situation the observed reduction of the shot noise may not be surprising.

[1] L. Chen, D. T. Lowder, E. Bakali, A. M. Andrews, W. Schrenk, M. Waas, R. Svagera, G. Eguchi,

L. Prochaska, Y. Wang, C. Setty, S. Sur, Q. Si, S. Paschen, and D. Natelson, Shot noise in a strange metal, Science **382**, 907 (2023).